ELSEVIER

Bioelectrochemistry 51 (2000) 53–65

Bioelectrochemistry

www.elsevier.com/locate/bioelechem

# Correction of the influence of baseline artefacts and electrode polarisation on dielectric spectra

John E. Yardley [a], Robert Todd [b], David J. Nicholson [a], John Barrett [a], Douglas B. Kell [a], Christopher L. Davey [a,*]

[a] *Institute of Biological Sciences, University of Wales, Aberystwyth, Ceredigion, Wales SY23 3DA, UK*
[b] *Aber Instruments, Science Park, Aberystwyth, Ceredigion, Wales, SY23 3AH, UK*

Received 28 January 1999; accepted 1 October 1999

**Abstract**

The deconvolution of biological dielectric spectra can be difficult enough with artefact-free spectra but is more problematic when machine baseline artefacts and electrode polarisation are present as well. In addition, these two sources of anomalies can be responsible for significant interference with dielectric biomass measurements made using one- or two-spot frequencies. The aim of this paper is to develop mathematical models of baseline artefacts and electrode polarisation which can be used to remove these anomalies from dielectric spectra in a way that can be easily implemented on-line and in real-time on the Biomass Monitor (BM). We show that both artefacts can be successfully removed in solutions of organic and inorganic ions; in animal cell and microbial culture media; and in yeast suspensions of varying biomass. The high quality of the compensations achieved were independent of whether gold and platinum electrodes were used; the electrode geometry; electrode fouling; current density; the type of BM; and of whether electrolytic cleaning pulses had been applied. In addition, the calibration experiments required could be done off-line using a simple aqueous KCl dilution series with the calibration constants being automatically calculated by a computer without the need for user intervention. The calibration values remained valid for a minimum of 3 months for the baseline model and indefinitely for the electrode polarisation one. Importantly, application of baseline correction prior to polarisation correction allowed the latter's application to the whole conductance range of the BM. These techniques are therefore exceptionally convenient to use under practical conditions. 

*Keywords:* Dielectric spectroscopy; Baseline artefacts; Electrode polarisation; Biomass estimation

## 1. Introduction

The study of the radio frequency dielectric properties of biological materials, and of cell suspensions in particular, has begun to encompass both the academic study of cell structure [1,2] and increasingly, its application to the monitoring of cellular biomass in industry [3–7]. The monitoring of biomass (live rather than dead cells) is a problem common to all cell culture systems and is critical as it provides a measure of the quantity of biocatalyst present if product formation is of interest, or of the cells themselves if they are to be harvested. In addition, there has been research on the application of the same basic technologies for medical research with several papers appearing, for instance, on whole human blood applications [8,9].

It is the understanding of the fundamental dielectric properties of cells and their constituent parts that is critical to the interpretation of the data obtained from both the industrial and medical measurements. However in the past, most of the research on basic cellular dielectrics has been done under rather artificial conditions to compensate for the limitations of the instruments at that time. The high conductivities of most biological fluids/growth media resulted in large instrument artefacts due to electrode polarisation and baseline distortions. To negate these, the cells were often suspended in low-conductivity media at very high cell concentrations [10]. Both these factors and the preparation time required to wash and resuspend the cells meant that the resulting dielectric data were not of physiological relevance. If one wishes to understand the industrial and medical dielectric data then one must be able to do basic dielectric studies under physiological conditions without sample preparation. Thus, the development of

* Corresponding author.

0302-4598/00/$ - see front matter 
PII: S0302-4598(99)00069-0

dielectric spectrometers that can cope with real biological milieu and which have mechanisms to compensate for baseline and electrode effects becomes of key importance for the future applications of dielectrics in basic research and industry.

Several dielectric spectrometers are currently used for biological measurements and most of these use existing or modified spectrometers produced by Hewlett–Packard [5,6,11–13]. However, one commercially available machine, the Biomass Monitor (BM), was developed from scratch for biological applications [3,14]. One of the important features of this machine is the fact that it uses a four-terminal electrode arrangement to reduce electrode polarisation [3]. This system is very effective when compared to, say, a pair of platinum–blacked platinum pin electrodes but does not remove all the polarisation in highly conducting media [10,15]. The BM's major use is for rapid, on-line and real-time (dielectric) biomass measurements in laboratory and industrial fermentation systems on a wide variety of cell types [3,4,7,16–18]. As it was developed to cope with measurements under physiological conditions, it is also a useful instrument for use in basic research [8,19,20].

Biological dielectric properties have been studied since the last century and have been reviewed by a number of authors [1,2,21–23]. Full details of how these and the physics behind them relate to biomass measurements can be found in [2,3,24,25]. However, for the purposes of this paper, a simplified description will suffice.

A suspension of cells can be regarded as having three components. Within the (spherical) cells and surrounding them are conducting aqueous ionic media, the cell's cytoplasm and the suspension medium, respectively. Surrounding the conducting core of the cell is the cell's plasma membrane which is essentially non-conducting. Thus, electrically the cell suspension can be regarded as a suspension of spherical capacitors, containing a conducting matrix and surrounded by a conducting medium. Below an applied electric field frequency of approximately 0.1 MHz, the cell membrane has a low admittance, resulting in the current flowing around the cells. As the cellular membrane capacitance is nearly fully charged, the net capacitance of the suspension is high. Correspondingly, the greater the volume fraction of cells, the greater is the capacitance of the suspension. Only intact cells give rise to a significant capacitance, as non-biomass material and necromass either lack membranes or membrane integrity. At frequencies over 1 MHz, the membrane admittance starts to increase significantly resulting in a marked reduction in the charging of the membrane capacitance and by 10 MHz, the capacitance of the suspension approaches that of the water in the suspending medium.

Thus, the capacitance of the suspension goes from a high low–frequency plateau to a low high–frequency one (Fig. 1). The frequency when the fall in capacitance (magnitude $\Delta C$) is half completed is called the characteristic

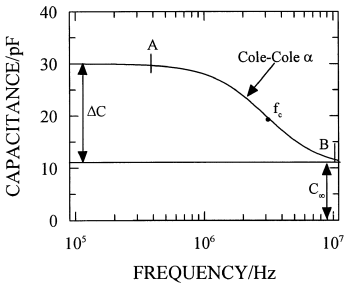


Fig. 1. The capacitance of a cell suspension in the frequency range of the β-dispersion. The height of residual high-frequency capacitance plateau is called $C_\infty$ while the height of the low-frequency plateau above this is called the capacitance increment ($\Delta C$). The frequency when the fall in capacitance is half complete is called the characteristic (or critical) frequency ($f_c$) and the rate of this fall is characterised by its Cole–Cole $\alpha$ value. In order to measure the biomass content of the suspension, one needs the value of $\Delta C$. To find this, the capacitance is measured at two spot frequencies, one on the low-frequency plateau (A) and the other on the high frequency plateau (B). When the latter's capacitance is subtracted from the former's, $\Delta C$ is obtained. This forms the basis of the dual-frequency method of biomass measurement.

frequency ($f_c$). This fall in capacitance as a function of increasing frequency is termed the β-dispersion and it is the size of its $\Delta C$ that increases with increasing biomass concentration. Thus, biomass estimation becomes a matter of measuring the magnitude of the $\Delta C$ of a suspension's β-dispersion. This is done either by recording the height of the low–frequency plateau at a single frequency or by taking the difference between capacitance values at two frequencies, one on either plateau. Typically, the frequencies used in recording biomass are 0.4 and 10 MHz, lines A and B, respectively on Fig. 1. The position of the $f_c$ of the β-dispersion is dependent upon the conductance of the suspension medium, the conductance of the cell cytoplasm, the cell size and the electrical properties of the plasma membrane [1]. During a fermentation, the suspending medium conductance can change markedly due to the cell's metabolic activity and the pH control regime, while the other cellular characteristics usually remain constant. Increases in suspending medium conductance cause the $f_c$ to move to a higher frequency, if the medium conductance falls, the $f_c$ drops to a lower frequency. Neither changes in the suspending medium conductance nor the accompanying movement of the $f_c$ change the real $\Delta C$ of the β-dispersion, but can affect the estimate of $\Delta C$ used for biomass estimations made using one or two frequencies [24].

To gain the maximum information about a cell suspension, it is important to do frequency scans of the dispersion. One can then fit these data to the Cole–Cole equation for permittivity; which models the shape of dispersions, to get best fit values for $\Delta C$, $f_c$ and $C_\infty$ [1,2,20]. These values can then be used with the appropriate cell suspension equations to calculate, among other things, the cellular membrane capacitance and cytoplasmic conductivity [8,20]. Indeed, many of the future developments of dielectric

technology will depend on detailed studies of such spectra and the physical models that relate them to the electrical properties of the cellular components. Not only will this improve fermentation monitoring but will open the way for novel methods to study cellular physiology which will ultimately result in new human/veterinary diagnostic technologies [8,26].

Two artefactual sources of capacitance have always hampered measurements in the radio–frequency range. These are electrode polarisation (below 1 MHz) and the increasing importance of cross-talk (the influence of conductance on the capacitance readings) as the frequency increases above a few MHz. On the BM, gain and offset effects are also important. All these effects in the context of the BM will be considered in the relevant parts of Section 2. Discussions of electrode polarisation with respect to biological dielectric measurements can be found in [15,27–30]. Electrode polarisation can cause serious problems and has until now limited detailed dielectric studies of cells under physiological conditions. This is unfortunate as it is believed that many pertinent bioelectrical effects occur at the frequencies where electrode effects dominate the spectra [31]. Therefore, robust on-line methods of reducing, or correcting for, electrode polarisation present in dielectric spectra are required to ensure accurate biomass estimations and the acquisition of reliable dielectric spectra.

As the BM's baseline is not completely flat as a function of frequency and as these distortions can depend on the conductance of the medium being measured, one can get erroneous $\Delta C$ (biomass) values being recorded during a fermentation as the broth conductance changes. When the cell concentration is high this is seldom a problem but it becomes a limiting factor for low biomass fermentations in highly conducting growth media [32]. In addition, dielectric spectra of β-dispersions can become severely distorted, particularly at high frequencies with highly conducting media where cross-talk can cause baseline errors (typically, a progressive decrease in capacitance as frequency increases). This in turn prevents the study of those subtle features of dispersion curves which encode much information of potential value in fermentation monitoring, cell physiology and medical diagnostics.

Several authors have discussed the correction of electrode polarisation and/or baseline artefacts on dielectric spectrometers [12,13,22,33] but this has only been done in detail for electrode polarisation on the BM [3,20,34,35]. Therefore in this paper, we aim to address baseline artefact problems and electrode polarisation in the context of the BM, although as will be emphasised in the relevant sections of this paper, the methods developed do have wider applicability. The approach taken to correct the data is: first, the use of a mathematical model of the baseline artefacts for data correction and then, the use of a model of the electrode polarisation to reduce its contribution to the final spectra. Primarily, we demonstrate the utility and robustness of a new baseline model of the BM (R.Todd and C. Davey, unpublished result), and in the process, the ''2f'' method of removing electrode polarisation from dielectric spectra outlined in Refs. [34,35] is tested using a newer version of the BM, with different electrode geometries and under a wider range of conditions.

## 2. Theory

### 2.1. Baseline flattening

The model for baseline flattening can be separated into two stages: setting up the calibration data and then applying them to real spectra. Both stages can be automatically carried out by a computer.

#### 2.1.1. Calibration stage

*2.1.1.1. Description of the baseline model.* Observation of the uncorrected response of the BM using discrete capacitors and resistors shows several distinct measurement artefacts; although these are usually small, they can be significant for some applications. With a low, near-zero, test capacitance, some frequency–dependence is observed in the baseline plot of capacitance vs. frequency. With a higher test capacitance, some variation of the gain of the capacitance measuring system becomes apparent in addition to the baseline offset above. Further, the addition of a test conductance gives rise to a capacitance error (cross-talk) which depends on both frequency and measured conductance.

The gain of the BM's capacitance measuring system is stabilised against temperature, frequency and cable effects by a feedback loop. However, there are a few input components which affect gain and which lie outside this control loop and can therefore cause gain variation and in particular, its variation with frequency.

The zero setting of the capacitance measuring circuitry is also feedback-stabilised but stray capacitance coupling around the input circuitry and in the probe inevitably produces some uncorrected error. An important factor which makes this error frequency-dependent is the frequency dependence of the permittivity of some of the materials used in the probe. Such sub-component dispersions were indicated in the manufacturer's literature and verified experimentally.

Cross-talk errors (the sample conductance affecting the measured capacitance) arise from three main effects. (i) Phase error in the measurement system: although tightly controlled, there are still residual phase errors (typically, only a few thousandths of a degree at the lower measuring frequencies) which cause errors approximately proportional to measured conductance. (ii) Stray inductive coupling in the probe circuit: this causes phase effects which result in errors proportional to $(\text{conductance})^2$. (iii) Electrode polarisation—see Section 2.2.

With very low conductivity samples, a further error appears due to the loading of the voltage electrodes by the shunt capacitance and conductance of the voltage amplifier circuit. This is not generally a problem at working conductances in fermentors, but it can complicate some calibration processes.

Initially, the baseline artefacts were modelled analytically with the expected theoretical functions of frequency and conductance [24]. Even though this model was experimentally verified, it was clear that it was far too complicated and time consuming to be of practical use. However, the insights gained with the resistor/capacitor studies allowed us to model the gross effects of each baseline artefact, at a given frequency, in terms of a series of additive and multiplicative effects. In this case, the model applies at a given single frequency, one just reapplies it at each frequency of interest. It is this model that is used in this paper. As the model treats each artefact as an additive or multiplicative term, it can, in principle be applied to other dielectric spectrometers provided that similar resistor/capacitor experiments to those above indicate that this model is applicable to the machine at all of the frequencies of interest.

The basic form of the mathematical model relating the measured (subscript m) capacitance ($C$) and conductance ($G$) values to the actual undistorted values (subscript a) is Eq. (1).

$$C_{\mathrm{m}}^{\omega \mathrm{G}} = \left( \frac{C_{\mathrm{a}}}{k_1^{\omega}} \right) - k_0^{\omega} - \left( k_2^{\omega \mathrm{G}} G_{\mathrm{m}}^{\omega} \right) \quad (1)$$

The superscripts ω and G indicate that the terms are at a given frequency and (measured) conductance, respectively. As outlined later, the actual capacitance values ($C_{\mathrm{a}}$) of the materials used for the calibration are constants. However, one should remember that when Eq. (1) is used to convert measured dispersion capacitance values to their undistorted forms, then the changes in $C_{\mathrm{m}}$ result in $C_{\mathrm{a}}$ also becoming a function of frequency (see Section 2.1.2).

All the capacitance ($C$) terms in Eq. (1) are in pF and the conductance term ($G$) is in mS. $k_1^{\omega}$ is a frequency-dependent (inverse of a) gain term and is dimensionless. $k_0^{\omega}$ is a frequency-dependent offset in the BM baseline and has units of pF. $k_2^{\omega \mathrm{G}}$ is the cross-talk term and has units of pF $\mathrm{mS}^{-1}$, thus $k_2^{\omega \mathrm{G}}\ G_{\mathrm{m}}^{\omega}$ is the cross-talk error (in pF) at a given frequency and conductance. The aim of the calibration stage is to quantify these three $k$ terms.

*2.1.1.2. Finding $C_a$.* $C_{\mathrm{a}}$ is the true physically correct capacitance value for the sample under test. The relative permittivity of KCl solutions are frequency-independent over the BM's frequency range and have a dielectric decrement compared to pure water of only −2.2 relative permittivity units for the maximal KCl concentration used here (approximately 200 mM) [21]. In the BM's most sensitive mode (''low'' cell constant mode) the cell constant is about 60 $\mathrm{m}^{-1}$ giving, by Eq. (2), the maximal change in capacitance due to the KCl of only −0.3 pF.

$$C = \varepsilon' \varepsilon_0 / M \quad (2)$$

where $C$ is the capacitance in Farads, $\varepsilon'$ is the (real part of the) relative permittivity of the dielectric, $\varepsilon_0$ the permittivity of free space ($8.854.10^{-12}$ F $\mathrm{m}^{-1}$) and $M$ is the geometric cell constant ($\mathrm{m}^{-1}$) measured as in Ref. [35]. Thus, the capacitance of all the KCl solutions is taken as that of pure water.

To calculate the constant $C_{\mathrm{a}}$ value to use in Eq. (1), one must know the cell constant of the electrode used and the temperature at which the experiments were done as temperature effects the permittivity of water. The permittivity of water from 0 to 50°C follows the following straight-line relationship (from a linear fit to data in Ref. [36]).

$$\varepsilon'_{\mathrm{H_2O}} = 87.63 - 0.36\,T \quad (3)$$

In this equation, $T$ is the temperature in °C. Thus, the $C_{\mathrm{a}}$ value to use for all the KCl calibration solutions at all the frequencies (at a given BM cell constant) was found by substituting the temperature at which all the calibrations were done into Eq. (3). The permittivity of water ($\varepsilon'_{\mathrm{H_2O}}$) was then inserted into Eq. (2) along with the relevant cell constant to give the $C_{\mathrm{a}}$ value.

*2.1.1.3. Calculate $k_1^{\omega}$.* To find $k_1$ as a function of frequency, one uses a special dummy probe instead of the usual BM electrode. This probe consists of a resistor–capacitor network that has been designed to produce $C$ and $G$ combinations that are independent of frequency in the BM's frequency range. The dummy probe is set to a low $G$ value (about 4 mS in low cell constant mode) and frequency scans carried out at the predefined frequencies (see Section 3) with its capacitance set to a low and high capacitance setting (about 50 and 100 pF, respectively in low cell constant mode). At this low $G$, the cross-talk term in Eq. (1) becomes negligible and so the low and high capacitance scans (subscripts L and H, respectively) can be written as:

$$C_{\mathrm{mL}}^{\omega} = \left( \frac{C_{\mathrm{aL}}}{k_1^{\omega}} \right) - k_0^{\omega} \quad (4)$$

$$C_{\mathrm{mH}}^{\omega} = \left( \frac{C_{\mathrm{aH}}}{k_1^{\omega}} \right) - k_0^{\omega}. \quad (5)$$

Subtracting Eq. (4) from Eq. (5) gives on simplification:

$$\mathrm{Gain}^{\omega} = \frac{1}{\mathrm{k}_1^{\omega}} = \frac{\mathrm{C}_{\mathrm{mH}}^{\omega} - \mathrm{C}_{\mathrm{mL}}^{\omega}}{\mathrm{C}_{\mathrm{aH}} - \mathrm{C}_{\mathrm{aL}}} \quad (6)$$

Eq. (6) shows that the Gain (and $k_1^{\omega}$) gives a measure of the change in measured capacitance to the actual real capacitance change at a given frequency. $C_{\mathrm{aH}} - C_{\mathrm{aL}}$ is a frequency-independent constant and can be calculated at 0.2 MHz where the BM's Gain is 1.0 (i.e., the actual and

measured capacitance changes are equal). Using this calculated value, the Gain and hence, $k_1^{\omega}$ can be found at each of the predefined frequencies.

*2.1.1.4. Calculate $k_0^{\omega}$.* To find $k_0$ at each of the predefined frequencies, one uses a scan of a single low KCl concentration solution. This KCl concentration is chosen to be above the very low conductance region where additional machine artefacts are known to occur due to the electrode's shaft impedance. For a standard (14 cm) length 25 mm diameter BM probe, 10 mM KCl is usually used for high and low cell constant measurements. At this low $G$, the cross-talk term of Eq. (1) is again negligible and Eq. (1) becomes on rearrangement:

$$k_0^{\omega} = \frac{C_a}{k_1^{\omega}} - C_m^{\omega}. \quad (7)$$

$C_m^{\omega}$ is the capacitance measured at each frequency on the low $G$ KCl solution; $C_a$ is the constant actual capacitance of the solution calculated earlier and $k_1^{\omega}$ at each frequency was also calculated above. Thus, one can calculate the $k_0^{\omega}$ value at each frequency.

*2.1.1.5. Calculate $k_2^{\omega G}$.* The cross-talk factor $k_2$ is a function of both frequency and conductance but it only makes a large contribution to the measured capacitance values at high frequencies with large conductances. To get $k_2$ as a function of both frequency and (measured) conductance, one uses scans of a series of aqueous KCl solutions that cover the BM's entire conductance range. The $k_2$ values are then calculated using Eq. (1) rearranged to give $k_2^{\omega G}$. The $C_a$ value needed was calculated earlier and is used for all the KCl solutions at all the predefined frequencies. $k_0^{\omega}$ and $k_1^{\omega}$ were estimated above at each predefined frequency and so by inserting the measured capacitance ($C_m^{\omega G}$) and conductance ($G_m^{\omega}$) values one gets $k_2$ as a function of both frequency and conductance ($k_2^{\omega G}$). To make this 2D calibration useful, two arrays of values are set up (Fig. 2a and b).

Both arrays have columns equivalent to the predefined frequencies in order from the lowest (0.2 MHz) to the highest (10 MHz). The rows in the arrays are equivalent to the scans of the individual KCl solutions in concentration (conductance) order from the lowest to the highest. However, the contents of the locations in the two arrays differ. Array (a) contains the measured conductance values ($G_m^{\omega}$) for each KCl calibration scan. Array (b), however, contains the equivalent $k_2^{\omega G}$ values calculated as described above.

There is a problem with the $k_2^{\omega G}$ values as they stand. At high conductances, the capacitances measured for the KCl solutions below 1 MHz will be much higher than expected due to electrode polarisation. As $C_a$ was calculated from physical principles, $k_1^{\omega}$ using a dummy probe which by definition has no electrode polarisation, $k_0^{\omega}$ using a low $G$ solution where the electrode effects are minimal,

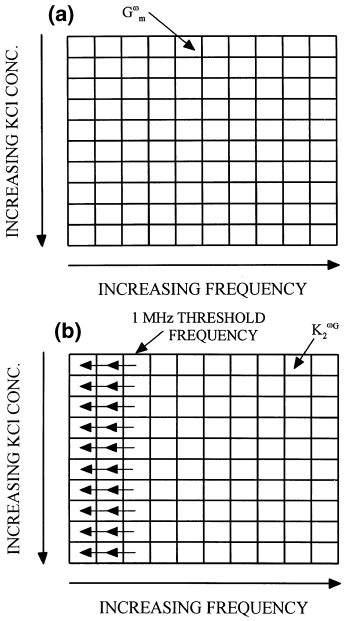


Fig. 2. A diagrammatic representation of the computer arrays used to obtain by linear interpolation the $k_2$ values to use at a measured conductance at each of the predefined frequencies when applying baseline compensation to experimental data. For clarity, the array contents are not explicitly shown and fewer frequencies and KCl concentrations than are typically used are also illustrated. Each row of the arrays corresponds to one KCl calibration scan at each of the predefined frequencies (columns). The concentration of the KCl calibration solutions used increases (in order) from top-to-bottom while the frequencies increase (in order) from left-to-right. (a) Array contents are the measured conductance ($G_m^{\omega}$) values for each of the KCl calibration scans. Thus, the arrowed location in (a) is the measured conductance of the lowest KCl concentration at the fifth lowest frequency. (b) Array contents are the $k_2^{\omega G}$ values equivalent to each of the scans of the calibration solutions. Also shown on (b) is a threshold frequency where electrode polarisation no longer significantly influences the $k_2$ data. $k_2$ values at this frequency are copied back over those at lower frequencies (indicated by the horizontal arrows) to prevent electrode polarisation from influencing the baseline calibration. See the text for a full discussion.

then one sees that it is the $k_2^{\omega G}$ values that will contain the distortions due to polarisation. Fortunately, the $k_2$ values at frequencies below 1 MHz are small and constant so that one may remove the polarisation's contribution to these calibration data by copying the $k_2$ values at this 1 MHz threshold (for each scan) back over the values at the lower frequencies, as is shown on Fig. 2b.

*2.1.2. Applying the calibrations to experimental data*

The aim of this stage is to take experimentally measured capacitance and conductance data (at the predefined frequencies) which are distorted by the baseline artefacts and correct them to give the actual physically correct values. Both the capacitances and conductances measured will now vary with frequency and conductance because of the dispersive nature of the material being measured in addition to the baseline artefacts. This in turn means that the actual capacitance terms will also become functions of

frequency and conductance. Thus, in the rearranged form of Eq. (1) below the ω and G superscripts now allow for the additional dependencies due to the sample under test (signified by the subscript s).

$$C_{as}^{\omega G} = k_1^{\omega}\left(C_{ms}^{\omega G} + k_0^{\omega} + k_2^{\omega G} G_{ms}^{\omega}\right) \quad (8)$$

Thus, for a given measured dispersion one takes each frequency point in turn and converts the measured data pair $C_{ms}^{\omega G}$, $G_{ms}^{\omega}$ for the sample under test and corrects it to $C_{as}^{\omega G}$ as follows.

(a) $k_0^{\omega}$ and $k_1^{\omega}$ at the given frequency are looked up from the previously calibrated data.

(b) The column corresponding to the relevant frequency is selected in array Fig. 2a and the contents of the array locations read to find the pair of locations where the (calibration) conductances sit at either side of the experimental sample's $G_{ms}^{\omega}$. This pair of array locations along with the equivalent pair in the array on Fig. 2b are used to linearly interpolate the $k_2^{\omega G}$ value to use for this frequency and measured $G_{ms}^{\omega}$ value.

(c) The values are substituted into Eq. (8) to give the corrected sample capacitance at that frequency ($C_{as}^{\omega G}$).

### 2.2. Electrode polarisation deletion: the ''2f'' method

In Ref. [35], it was shown that electrode polarisation measured on a BM follows the power law form previously observed by other groups (on other instruments using different electrode arrangements):

$${}^{f}C_p = {}^{1\,Hz}C_p f^p \quad (9)$$

where ${}^{f}C_p$ is the capacitance (in pF) due to electrode polarisation at a given frequency ($f$ in Hz), ${}^{1\,Hz}C_p$ is numerically equal to the polarisation capacitance at 1 Hz and $p$ is a dimensionless power term.

To make this model easier to relate to the polarisation seen on BM spectra, it was reformulated into more intuitive terms. The lowest frequency used during a scan was called ${}^{L}f$ ($2 \times 10^5$ Hz on a BM) and the capacitance due to electrode polarisation at that frequency was called ${}^{L}C_p$. This latter provides an intuitive measure of the magnitude of the polarisation on the spectrum. The frequency when ${}^{L}C_p$ had halved was called the ''half frequency'' (${}^{h}f$, this is not a half-life) and was found to be a constant of $2.8 \times 10^5$ Hz (relative to a ${}^{L}f$ of $2 \times 10^5$ Hz) for BMs.

In Ref. [34], this constant ${}^{h}f$ was exploited to produce a simple method to estimate the frequency dependence of the polarisation which could then be subtracted from the suspension spectrum to leave polarisation free data. To do this, the capacitance of the spectrum (in pF) was measured at ${}^{L}f$ and ${}^{h}f$ to give ${}^{L}C_m$ and ${}^{h}C_m$, respectively. These values were then inserted into Eq. (10) and the capacitance due to the polarisation (${}^{f}C_p$) at each spectral measuring frequency ($f$) calculated.

$${}^{f}C_p = 2\left({}^{L}C_m - {}^{h}C_m\right)2^n \quad (10)$$

where $n$ is given by:

$$n = \frac{\log\left({}^{L}f/f\right)}{\log\left({}^{h}f/{}^{L}f\right)}. \quad (11)$$

Subtraction of the ${}^{f}C_p$ value at each frequency from the suspension data results in data largely free from electrode polarisation. The formula relating errors in the sample measurements to errors in the calculated electrode polarisation is given in Ref. [34]. In addition, this reference outlines modifications to the model which gives it a very broad application to other spectrometer and electrode configurations.

## 3. Methods

### 3.1. Chemicals and organisms used

All of the reagents used were of analytical grade and suspensions/solutions were prepared with distilled water. *Saccharomyces cerevisae* was obtained locally as a paste and was slurried in 100 mM KCl prior to use, and always used the same day. Dry weights were made on the actual sample being scanned by first filtering as in Ref. [20] and then drying at 100°C in an oven to constant mass.

### 3.2. Electrodes and their preparation

Unless stated otherwise, the same 25 mm diameter standard Aber Instruments (Science Park, Aberystwyth, Wales, UK) biomass probe was used throughout. This electrode type consists of a 14 cm long cylindrical plastic shaft (25 mm in diameter) which has four coplanar platinum pin electrodes projecting from one end.

The electrodes were always stored dust free and dry and before each experiment, they were thoroughly cleaned as in Ref. [35], in order to remove any fouling material (no electrolytic cleaning was used). During the experiments, the probes were never allowed to dry-out, and at such points when recording of dielectric data was halted, the probes were suspended in distilled water. Cell constant measurements were made using the methods in Ref. [35] and for the probe above were 0.61 $cm^{-1}$ in BM low cell constant mode and 1.0 $cm^{-1}$ in high mode.

### 3.3. Electrical measurements

The dielectric spectra were recorded using the same Biomass Monitor 214A (admittance domain) dielectric spectrometer (Aber Instruments) which was a more modern version of that used in Refs. [34,35]. The instrument was set up and switched on several hours in advance of the experiments to ensure that the electronics were stabilised.

Unless stated otherwise, the instrument was configured as follows: low pass filtration off, single frequency/scanning mode active, both display and output set to absolute capacitance (''C mode''), high cell constant mode and with the electrolytic cleaning system deactivated. All the experiments in this paper were done in both the high and low cell constant BM modes, however, for brevity only the high cell constant data are shown. In all the experiments, the low cell constant data mirrored the high cell constant ones even to the extent that the measured $^{h}f$ values were identical.

The experiments were run under computer control using an ''in-house'' programme called BMScan. This was written in the Microsoft QuickBasic 4.5 compiler and installed on a 486/66 MHz IBM compatible PC. Data transfer was via a DT2811 PGH A/D, D/A converter card (Data Translation, The Mulberry Business Park, Wokingham, Berkshire, RG41 2GY UK). During each experiment, the programme was configured to scan the BM through the same predefined 50 frequencies in the same randomised order. The 50 frequencies were chosen to be evenly distributed along a log frequency axis between 0.2 and 10 MHz and to include any frequency sub-sets that might be used for later scanning experiments. In addition, the $^{L}f$ and $^{h}f$ values for the polarisation deletion 2f method were included, as was the 1 MHz threshold frequency used to calculate $k_2$. While scanning, a delay of 4.5 s was used after each frequency change, to allow the electronics to settle, prior to taking and averaging 10 replicate readings each 0.1 s apart.

Unless stated otherwise, when the BM's electrolytic cleaning cycle was used, the complete cycle was manually applied 10 times in succession, only after that were any adhering gas bubbles shaken off the probes. The shaking was required as rather more pulses were applied, and hence, more bubbles formed, than is usual in a fermentation environment and the stirred beaker used lacked the shear forces that normally clear the bubbles in a working situation. Finally, the capacitance and conductance values at 0.2 MHz were allowed to stabilise before continuing to scan.

The experimental vessel was a 600 ml Pyrex beaker, containing 500 ml of the relevant solution or suspension. The BM's probe was positioned centrally in the liquid, so that the electric field produced did not couple significantly into the Pyrex or the magnetic stirrer bar (''flea''). A constant stirring speed of 300 rpm was maintained throughout, and the BM's head amplifier earth lead was connected to the metal top of the magnetic stirrer box [24].

### *3.4. Baseline and electrode polarisation calibration experiments*

The calibration experiments consisted of frequency scans of KCl solutions of differing conductances (i.e., concentrations) covering the BM's entire conductance range. A different set of scans was used for the high and low cell constant modes of the BM for each type of electrode used. The starting concentration was 10 mM KCl, this conductance being above a level where probe shaft impedance effects were a problem with the standard 25 mm probes, and was also a convenient concentration for the estimation of the cell constants. The remaining solutions used were made up so that the measured conductances at 1 MHz were about 0.5 mS apart.

The $^{h}f$ values for the electrodes were estimated exactly as in Ref. [35] and did not rely on the application of the baseline flattening model as a preliminary step so that the two methods could be evaluated together without being interlinked. Although in a real system, one would do a full baseline correction prior to determining the $^{h}f$.

### *3.5. Electrode polarisation controls*

As a control, the previous standard method of electrode polarisation removal used for BM measurements was used [15]: electrode polarisation control subtraction. This involved recording the conductance of the suspension at the lowest frequency used and then adjusting a sample of the suspending medium to the same conductance (at the same frequency) using distilled water. The frequency scan of this control was then subtracted from the suspension data to give a polarisation ''free'' spectrum.

## 4. Results and discussion

The aim of this paper is to thoroughly test the baseline flattening model, and to elaborate on and strengthen the findings and results published in Refs. [34,35] on the 2f polarisation deletion method. In order to achieve this objective, a broad range of media were tested and the effect of the serial application of the baseline flattening method followed by the 2f polarisation deletion method were ascertained.

In order to apply the baseline flattening and polarisation deletion methods to experimental data, a programme called c_baseln.exe was written in-house (in Microsoft QuickBasic) and installed on a 486/66 MHz IBM compatible PC. The programme consisted of two parts. First, it could be supplied with a series of KCl calibration scans of increasing conductance to allow it to generate arrays of $k_0$, $k_1$ and $k_2$ values as described in Sections 2 and 3. Secondly, experimental scans could be fed to the program which then automatically applied baseline flattening and then optionally 2f polarisation deletion to the data (see Section 2). For each probe type in each of the BM cell constant modes (high or low) tested a new set of KCl calibration data (and hence, $k_0$, $k_1$ and $k_2$ values) were generated. The ''half-frequency'' ($^{h}f$) required for the 2f polarisation deletion method (see Section 2) was ascertained from these same KCl calibration data exactly as in Refs. [34, 35] using an

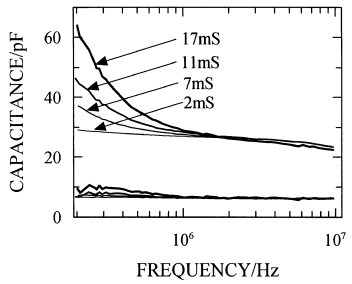


Fig. 3. The effect of increasing the concentration (and hence conductance, $G$) of an aqueous sodium chloride solution on the capacitance spectrum measured by a BM. The upper group of curves are scans of NaCl solutions at the (1 MHz) conductances indicated. The application of baseline flattening using the previously measured values for $k_0$, $k_1$ and $k_2$ (which enveloped but did not specifically include these measured conductances), followed by 2f polarisation deletion resulted in the lower set of capacitance scans. For all the conductances over all the frequencies, the capacitance data were virtually frequency independent at the capacitance of about 7 pF expected for NaCl solutions at this temperature.

${}^{\mathrm{L}}f$ of 0.20 MHz, and gave a value of ${}^{\mathrm{h}}f$ of 0.28 MHz. These calibration data provided good baseline flattening for up to 3 months (up to 8 months was seen in one previous study, data not shown) while the polarisation deletion method's ${}^{\mathrm{h}}f$ was completely independent of experimental and instrumental conditions and of time. In all the experiments described below the relevant $k_0$, $k_1$ and $k_2$ values obtained from the calibration KCl solutions were used to compensate the spectra of a wide variety of media (including other KCl solutions) to study the applicability of such a simple calibration regime to media/media components likely to be encountered in real fermentations and physiological studies.

In order to study the effects of artefactual capacitance associated with salts, several aqueous solutions of inorganic ions were scanned and the data corrected using c_baseln.exe as described above. The compounds used were KCl, NaCl, $NH_4Cl$, $CaCl_2$, $KH_2PO_4$, $Na_2HPO_4$, $MgSO_4$ and $NH_4NO_3$. For each salt, a range of conductances were scanned by adding the solid salt to an initial 10 mM solution. In all cases, the conductances of these solutions as judged at 1 MHz did not include the conductances in the $k_2$ calibration array (see Fig. 2a).

The upper part of Fig. 3 shows the raw data for the NaCl solutions used during this experiment. As expected, as the conductance of the solution increased the magnitude of the capacitance rise below 1 MHz (electrode polarisation) increased [15]. The BM baseline was offset up some 22 pF from the theoretical value of just under 7 pF for a saline solution on this BM (calculated in the same way as $C_a$ in Section 2). The 2 mS solution shows the slight linear fall in the baseline with increasing frequencies due to the dispersion of some of the components used in the probe shaft. The increase in the tip-down (cross-talk) at high frequencies as the conductance increases is also clearly shown. One can see that if a small biological β-dispersion was measured under reasonably conducting conditions, then the combination of electrode polarisation and baseline distortions could severely limit the usefulness of the data, be they full scans or one- or two-frequency biomass measurements.

The lower set of flat lines on Fig. 3 is the result of applying first the baseline flattening and then the polarisation deletion method to the raw data using c_baseln.exe. The baseline has been pulled down close to the capacitance for a saline solution on this BM, and is virtually frequency- and conductance-independent as expected for salines in this frequency range. In all the non-biological experiments in this paper, the corrected capacitances were typically between 6.5 and 7.0 pF, i.e., very close to the expected value of just under 7 pF. As the NaCl conductances used in these experiments were chosen not to include those used to linearly interpolate the $k_2$ values in the calibration arrays (see Fig. 2), it is clear that this interpolation method works extremely well. All the salt solutions at all the conductances tested produced exactly the same quality of post-correction spectra. This demonstrates that both the polarisation deletion and baseline flattening methods are independent of the inorganic ions in solution.

To complement the data obtained from the inorganic ions, a variety of organic ions were scanned. The compounds used were 100 mM sodium acetate, 100 mM potassium acetate and 5% (v/v) lactic acid. Fig. 4 shows the sodium acetate data and once again the raw data deviates from the expected frequency independent spectrum of about 7 pF (i.e., close to that of water). As in Fig. 3, the effect of electrode polarisation below 1 MHz and the BM baseline distortions at higher frequencies are evident. Line A shows the effect of applying the baseline flattening to the raw data. This has resulted in the baseline being pulled down to the expected value and flattened, apart from the range below 1 MHz where electrode polarisation still distorts the spectrum. Line B is the fully compensated data generated by applying the polarisation deletion method to the line A data. The other organic ion solutions tested produced equally good results. Once again correction of

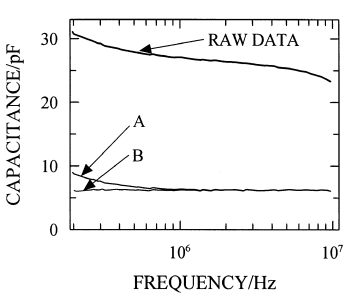


Fig. 4. The effect of baseline flattening followed by polarisation deletion on the dielectric spectrum of 100 mM sodium acetate. Line A is the result of applying baseline flattening to the raw data while line B shows the effect on the A data of applying the 2f electrode polarisation deletion method.

the data using the $k_0$, $k_1$ and $k_2$ values generated earlier using simple KCl scans was shown to be generally applicable. Leading on from the examination of individual ions in solution, we needed to consider how effective baseline flattening and 2f electrode polarisation deletion is in complex ionic mixtures.

In animal cell culture and microbiological media, the concentrations of univalent cations and anions dominate the total conductivity. Both the organic and inorganic ions previously scanned may be found in such media. Thus, it is important to study the effect of these complex mixtures on the two correction methods discussed here.

The animal cell media tested were, Roswell Park Memorial Institute (RPMI) 1640 medium (Labtech International) with and without L-glutamine; RPMI 1640 medium with 10% foetal calf serum; Minimum Essential Medium Eagle (MEME) (Sigma) with Hank's salts, sodium bicarbonate and L-glutamine; MEME (Sigma) without phenol red, L-glutamine and sodium bicarbonate; Dulbecco's Modified Eagle's Medium (MEM) (Life Technologies) without sodium pyruvate but with 400 mg/ml glucose; Hank's (Sigma) without sodium bicarbonate; Hank's (Sigma) without calcium chloride, magnesium sulphate and sodium bicarbonate; HEPES (*N*-[2-hydroxyethyl] piperazine-*N*′-[2-ethanesulfonic acid]) (Sigma) and Dulbecco's phosphate-buffered saline (Sigma).

Fig. 5 shows the effect of applying baseline flattening (A) followed by 2f polarisation deletion (B) to the raw dielectric spectrum of Hank's medium without sodium bicarbonate. The resulting spectrum (B) was frequency-independent at a value close to the 7 pF expected from theoretical considerations. All the other media tested produced equally good post-correction spectra.

The microbiological media scanned were 37 g/l Brain Heart Infusion (Oxoid); 13 g/l Nutrient Broth E (Oxoid); 33.4 g/l Czpapek Dox (Oxoid); 32.4 g/l Todd Hewitt Broth (LAB M); 1% w/v Yeast Extract (Difco Laboratories); 2% w/v Sabouraud (Merck); and 30 g/l Dextrose Broth (Merck).

From Fig. 6, one can see the effect of applying baseline flattening (A) followed by 2f polarisation deletion (B) to

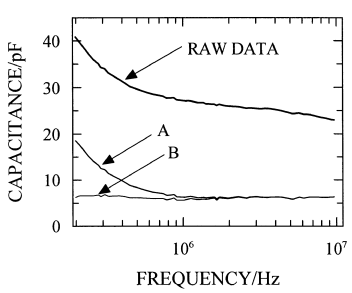


Fig. 5. The effect of applying baseline flattening (A) followed by 2f polarisation deletion (B) to the raw dielectric spectrum of a complex animal cell culture medium (Hank's medium without sodium bicarbonate). The resulting spectrum (B) was frequency independent at a value close to the 7 pF expected from theoretical considerations.

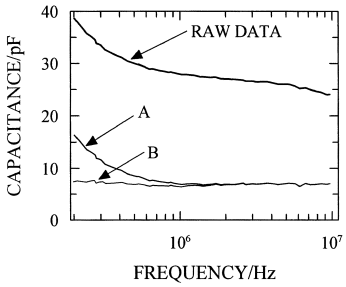


Fig. 6. The effect of applying baseline flattening (A) followed by 2f polarisation deletion (B) to the raw dielectric spectrum of a complex microbiological medium (Brain Heart Infusion). As expected, the resulting spectrum (B) was frequency independent with a value close to that of water/dilute protein solutions.

the raw dielectric spectrum of Brain Heart Infusion medium. As expected, the resulting spectrum (B) was frequency-independent with a value close to that of water/dilute protein solutions [21,22]. Once again all the other media tested produced equally good post-correction spectra. The results for both the animal and microbial media show that the baseline flattening and 2f methods effectively remove artefactual capacitance in complex mixtures.

From these previous experiments, it is the next logical step to examine the effects of baseline flattening and polarisation deletion on real cell suspensions. In these suspensions, the correction methods must remove the electrode polarisation and the baseline distortions without fundamentally changing the cell's β-dispersion curve. To this end, yeast suspensions with dry weights ranging from 36 to 125 mg $ml^{-1}$ were made–up in 100 mM aqueous KCl and scanned as described in Section 3. 100 mM was used as this provided both ''strong'' baseline and electrode polarisation artefacts without excessively stressing the cells. By varying the yeast concentration (biomass) of the suspensions and not the conductance of the suspending medium, we avoided exposing the yeast cells to varying osmotic stresses. Thus, we prevented variation in cell size and medium conductance from altering the $\Delta C$ and $f_c$ of the cell's β-dispersion [1].

Fig. 7 illustrates the effects of both baseline artefacts and electrode polarisation upon the scans. The inverted sigmoidal β-dispersion of the cells is clearly seen but it fails to plateau properly at low-frequencies due to the presence of electrode polarisation (below 1 MHz). By varying the yeast concentration, one can study the effect that varying the magnitude of the cell's dispersion in relation to the magnitude of the polarisation and baseline effects has on the baseline/polarisation deletion methods. This combination of electrode polarisation and baseline distortions greatly interferes with the interpretation of these data, particularly at low biomass concentrations.

Fig. 8 shows the combined effects of applying baseline flattening followed by polarisation deletion to the data

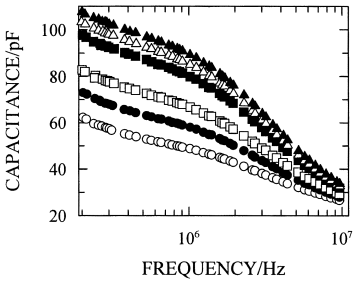


Fig. 7. The raw dielectric spectra of yeast suspensions made up of 100 mM KCl (from the top down, 125, 107, 94, 75, 51 and 36 mg $ml^{-1}$ dry weight). The inverted sigmoidal β-dispersion of the cell suspension is clearly seen but it fails to plateau properly at low-frequencies due to the presence of electrode polarisation. The BM's baseline distortions also result in some of the distortions seen.

from Fig. 7 using c_baseln.exe. The inverted sigmoidal β-dispersion curves of the cell suspensions are now clearly defined (at all cell concentrations) with a noticeable low frequency plateau as the electrode polarisation has been removed.

These results compare favourably to those produced by the previous standard technique for electrode polarisation compensation on the BM: namely, using the electrode polarisation control subtraction method [15]. Fig. 9 compares the raw suspension scan data (solid circles) for the 94 mg $ml^{-1}$ yeast suspension from Fig. 7 to the results of applying (i) baseline flattening followed by polarisation deletion (open circles) and (ii) of subtracting polarisation control data from the raw data (squares). The two sets of compensated data are similar, both with a well-defined low frequency plateau. The effect on the high frequency end of the spectrum is significant as the polarisation control subtraction method (squares) tends to result in a residual high frequency capacitance close to zero (although one can add back the calculated capacitance of water if required) while the other analysis methods (open circles) produce a more physically reasonable value. A better way to compare the two sets of data is to fit both to the Cole–Cole equation [37] which characterises a dielectric dispersion in terms of

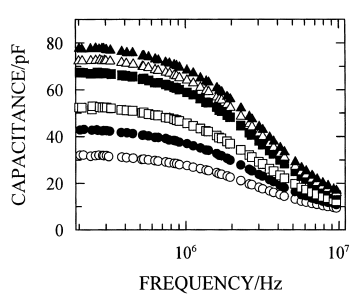


Fig. 8. The effect of the application of baseline flattening followed by 2f polarisation deletion on the dielectric spectra of the yeast suspensions shown in Fig. 7 (from the top down, 125, 107, 94, 75, 51 and 36 mg $ml^{-1}$ dry weight). The expected inverted sigmoidal β-dispersion curves of the cell suspensions are now clearly seen.

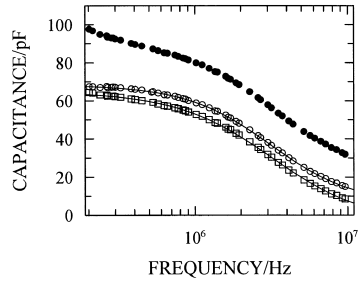


Fig. 9. A comparison of the effect on the raw 94 mg $ml^{-1}$ yeast spectrum from Fig. 7 (here, replotted as solid circles) of applying (i) baseline flattening followed by 2f polarisation deletion (open circles) and (ii) of subtracting polarisation control data from the raw data (squares). The two sets of compensated data are fairly similar, both with a well-defined low-frequency plateau. A better way to compare the two sets of data is to fit both to the Cole–Cole equation which characterises a dielectric dispersion in terms of its best fit values for $\Delta C$, $f_c$, Cole–Cole $\alpha$ and $C_\infty$ (see Fig. 1). The lines through the data are two such fits done using non-linear least squares curve fitting.

its best fit values for $\Delta C$, $f_c$, Cole–Cole $\alpha$ and $C_\infty$ (see Fig. 1). The lines through the data on Fig. 9 are two such fits done using non-linear least squares curve fitting using the Levenburg–Marquardt algorithm with ''unity (simple) weighting'' (see Refs. [8,20] for details). The best fit values for the square and open circle data, respectively, are: $\Delta C$ 70.8, 63.9 pF; $f_c$ 3.21, 3.13 MHz; Cole–Cole $\alpha$ 0.16, 0.10 and $C_\infty$ −5.4, 4.9 pF. The capacitance of the suspending medium is about 7 pF for these experimental conditions and it is clear that the $C_\infty$ of the open circle data is just below this value. This is in line with previous experiments showing a dielectric decrement relative to the suspending medium at these frequencies [2]. The most important effect is seen at high frequencies where the fact that the polarisation control subtraction method fails to fully compensate for the artefactual high–frequency baseline capacitance fall has resulted in the extrapolated value of $C_\infty$ being too low resulting in an artefactually elevated $\Delta C$ value. These results show that both polarisation compensation methods produce data that are comparable.

A further problem that needs to be examined as a consequence of introducing cells to the experiments is that of electrode fouling. This is known to represent a potential source of electrode polarisation variation during a fermentation process [24]. This can be due to the cells, their products or the components in the medium adhering to the electrodes as the environment changes during a fermentation. It is, therefore, essential to ensure the electrodes are kept clean, thus preserving consistent dielectric measurements. The BM has an in-built electrolytic cleaning cycle and this was applied as described in Section 3. Fig. 10 shows the effect of the serial application of 10 electrolytic cleaning pluses on the dielectric spectrum of 100 mM aqueous KCl. The labels ''pre'' and ''post'' refer to spectra taken before and after the application of the pulses, respectively. The upper pair of lines are the raw pre- and

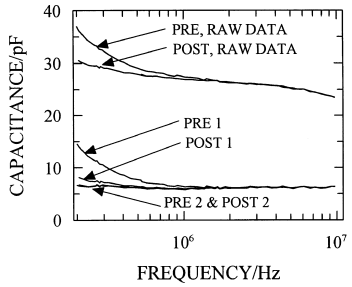


Fig. 10. The effect of the serial application of 10 electrolytic cleaning pulses on the dielectric spectrum of 100 mM aqueous KCl. The labels ''pre'' and ''post'' refer to spectra taken before and after the application of the pulses respectively. The upper pair of lines are the raw pre- and post-pulse data. As expected from previous experience, the cleaning pulses resulted in a significant fall in electrode polarisation but had no effect on the BM baseline artefacts. The lines pre-1 and pre-2 are the results of applying baseline flattening followed by 2f polarisation deletion, respectively to the pre-cleaning pulse raw data. Post 1 and post 2 are the equivalent data for the post-cleaning pulse data.

post-pulse data. As expected from previous experience, the cleaning pulses resulted in a significant fall in electrode polarisation, probably due to the removal of adhering material and exposure of clean electrode material [35]; however, it had no effect on the BM baseline artefacts. The lines pre-1 and post-1 are the results of the application of baseline flattening to their equivalent raw spectra. This resulted in the baseline being pulled down to the expected value of approximately 7 pF and flattened at all frequencies, although the continued presence of electrode polarisation still caused an increase in capacitance below 1 MHz. The lines pre-2 and post-2 are the result of the further application of the 2f polarisation deletion method. *Complete* compensation was achieved for electrode polarisation in the sub 1 MHz range with the resulting capacitance data being frequency-independent and close to 7 pF.

With some animal cell media containing serum, the cleaning pulses can actually cause electrode fouling by precipitating the protein onto the electrode surfaces (a process also seen in some beer worts). To test the effect of this on the baseline and polarisation corrections RPMI animal cell medium with 10% foetal calf serum was exposed to 10 cleaning cycles (without the subsequent shaking off of the bubbles) using the standard 25 mm probe. A frequency scan was then done with the precipitated matrix still on and across the probe pins. This process was repeated a further three times resulting in a fibrous protein and bubble matrix completely enveloping the four electrodes. All the scans gave a flat baseline after the application of the baseline correction and 2f methods. However, the corrected and raw data were noticeably more noisy and were increasingly offset-up as the number of applied cleaning cycles increased. After 40 pulses, this offset was some +15 pF on both the raw and corrected data. However, when the experiment was repeated but with the precipitate washed off after each block of pulses (prior to scanning), the raw and corrected scans lacked the progressive offset.

Up to this point, we have examined the effects of artefactual capacitance associated with the 25 mm diameter (short) probe with platinum electrodes. For completeness, this should be compared to another commercially available fermentation BM probe. This other probe is a 19 mm diameter, long version of the previously used probe type but with more closely spaced gold electrodes. Baseline artefacts are exacerbated by the very long probe shaft (26 cm) and the gold electrode pins are known to be more polarisable than platinum ones and so electrode polarisation is worse as well [35].

In order to test the baseline flattening and 2f methods, it was first necessary to generate fresh KCl calibration data for c_baseln.exe. These data were specific to the 19 mm probe and measured in both the low and high cell constant modes of the BM. A $^{h}f$ of 0.29 MHz was found for both cell constant modes, which is identical to that found for the 25 mm diameter probe (0.28 MHz) given that a BM only gives frequency in MHz to two decimal places. In addition, these values are the same as was found for the different probes used in Refs. [34,35] on an earlier version of the BM. A set of new experimental KCl solutions was scanned as was done previously (the $G$ values were not those used to generate the calibration $k_2$ values) and the spectra compensated using c_baseln.exe as before. In both low and high cell constant modes, the baseline was flattened at the value expected for a dilute saline solution and electrode polarisation was removed, leaving a flat baseline free from artefacts. Similar experiments giving the same results (including the same $^{h}f$ as found in all the previous experiments) were also obtained for a ''Mexican Hat'' probe (a commercial electrode produced by Aber Instruments which has the electrode pins confined to a 1 ml cavity [31]), an experimental 25 mm diameter probe with its electrodes flush with the probe's end, and a probe built flush onto the surface of a printed circuit board. Thus, the baseline correction and the 2f method work effectively with other probe types as well.

## 5. Concluding remarks

For truly physiologically relevant dielectric studies to be carried out, one must be able to do measurements without sample preparation, *in situ* if possible (e.g., in a fermentor or sample vessel), and with the cells at their natural concentrations in their actual maintenance media. Given the highly conducting nature of many biological materials, electrode polarisation and spectrometer baseline artefacts will severely limit the quality of the dielectric data and prevent subtle physiological effects from being detected. During fermentations, the medium conductance

often changes and this in turn means that the polarisation and baseline artefacts become time-dependent, which in turn can introduce time-dependent errors into one- and two-frequency biomass measurements. If these measurement artefacts can be eliminated, then this process would become both more reliable, more sensitive and more widely applicable (e.g., to low concentration animal cell cultures).

This paper tests a new method of flattening the BM's baseline as well as expanding on the observations made in Refs. [34,35] on the 2f polarisation deletion method. The pair of methods when used together were found to produce a substantial decrease in both the baseline and polarisation artefacts on the BM. In addition, the calibrations required by the methods could be done off-line using simple scans of KCl solutions. The resulting calibration data were stable over considerable lengths of time and so regular recalibration was not necessary. In addition, one can now recalibrate a BM for use with a wide variety of probe types without the need for the hardware changes required at the moment. Importantly, the methodologies could be applied to on-line measurements in real-time and were completely independent of the physical and chemical nature of the media being monitored.

In Refs. [34,35], it was found that the $^{h}f$ used by the 2f method becomes conductance-dependent below a few mS due to instrument baseline artefacts. The application of baseline flattening before applying the 2f method to the spectra eliminates this problem. Thus, the two methods are synergistic.

A significant finding is that in all the experiments (including those in Refs. [34,35]) with all the probes, the $^{h}f$ value (relative to 0.20 MHz) was constant. This was even the case between high and low cell constant modes on the BM which also alters the electrode surface current density (as do the different electrode geometries used), a factor known to influence the magnitude of electrode polarisation [15,29]. It thus appears that the 2f polarisation deletion method does not require any recalibration over time.

Although the two correction methods work well, they can leave a residual uncompensated capacitance of a couple of pF at low–frequencies when measurements are made at the *extreme* high-end of the BM's conductance range. However, this error is very small compared to the errors present prior to the application of the correction methods (see Fig. 3). If measurements are being made on cells suspended in media of *very* low conductance, then the β-dispersion's low–frequency plateau can occur at frequencies below the BM's frequency range. Under these conditions, the electrode polarisation is negligible but if one were to apply the 2f polarisation deletion method to these data, then the result would be a completely artefactual low–frequency β-dispersion plateau in the BM's frequency range. It is therefore important that one only applies the 2f deletion method to data where at least the very start of the low–frequency β-dispersion plateau is within the spectrometer's frequency range [34,35].

The combination of the baseline compensation and 2f polarisation deletion methods provides a new and highly satisfactory means for the deletion of artefactual capacitance, facilitating true on-line corrections to be made without the need for off-line destructive control experiments (e.g., the polarisation control subtraction method). This will now enable the BM to be used with confidence for low-density cultures in highly conducting media [32]. The ability to examine artefact free low–frequency dielectric spectra may ultimately lead to the ability to relate capacitance spectra to cell physiology and biochemistry. In the fermentation industry, this would permit accurate and sophisticated control strategies to be implemented, improving product quality, maximising productivity and helping in process optimisation. These results are also vital preliminary steps in the development of this technology for medically relevant studies and novel diagnostics.

## Acknowledgements

We would like to thank the BBSRC and the Wellcome Trust for financial support.

## References

[1] K.R. Foster, H.P. Schwan, Dielectric properties of cells and tissues: a critical review, CRC Crit. Rev. Biomed. Eng. 17 (1989) 25–102.
[2] C.L. Davey, D.B. Kell, The low–frequency dielectric properties of biological cells, in: Bioelectrochemistry of Cells and Tissues, Birkhäuser, Zurich, 1995, pp. 159–207.
[3] C.M. Harris, R.W. Todd, S.J. Bungard, R.W. Lovitt, J.G. Morris, D.B. Kell, The dielectric permittivity of microbial suspensions at radio-frequencies: a novel method for the estimation of microbial biomass, Enzyme Microb. Technol. 9 (1987) 181–186.
[4] C.A. Boulton, P.S. Maryan, D. Loveridge, The application of a novel biomass sensor to the control of yeast pitching rate, in: Proc. European Brewing Convention Congress, Zurich,1989, pp. 653–661.
[5] K. Mishima, A. Mimura, Y. Takahara, K. Asami, T. Hanai, On-line monitoring of cell concentrations by dielectric measurements, J. Ferment. Bioeng. 72 (1991) 291–295.
[6] K. Mishima, A. Mimura, Y. Takahara, On-line monitoring of cell concentrations during yeast cultivation by dielectric measurements, J. Ferment. Bioeng. 72 (1991) 296–299.
[7] R. Fehrenbach, M. Comberbach, J.O. Pêtre, On-line biomass monitoring by capacitance measurement, J. Biotechnol. 23 (1992) 303–314.
[8] H. Beving, L.E.G. Eriksson, C.L. Davey, D.B. Kell, Dielectric properties of human blood and erythrocytes at radio frequencies (0.2–10 MHz); dependence on cell volume fraction and medium composition, Eur. Biophys. J. 23 (1994) 207–215.
[9] A. Irimajiri, M. Ando, R. Matsuoka, T. Ichinowatari, S. Takeuchi, Dielectric monitoring of rouleaux formation in human whole blood: a feasibility study, Biochim. Biophys. Acta 1290 (1996) 207–209.
[10] C.L. Davey, D.B. Kell, R.B. Kemp, R.W.J. Meredith, On the audio- and radio-frequency dielectric behaviour of anchorage-independent, mouse L929-derived LS fibroblasts, Bioelectrochem. Bioenerg. 20 (1988) 83–98.
[11] K. Asami, T. Yonezawa, Dielectric behaviour of wild-type yeast and vacuole-deficient mutant over the frequency range of 10 kHz to 10 GHz, Biophys. J. 71 (1996) 2192–2200.

[12] S.A. Siano, Biomass measurement by inductive permittivity, Biotech. Bioeng. 55 (1997) 289–304.
[13] R. Bragos, X. Gamez, J. Cairo, P.J. Rui, F. Godia, Biomass monitoring using impedance spectroscopy, Ann. N.Y. Acad. Sci. 873 (1999) 299–305.
[14] C.L. Davey, R. Todd, J. Barrett, From concept to market in industrial impedance applications, Ann. N.Y. Acad. Sci. 873 (1999) 239–244.
[15] C.L. Davey, G.H. Markx, D.B. Kell, Substitution and spreadsheet methods for fitting dielectric spectra of biological systems, Eur. Biophys. J. 18 (1990) 255–265.
[16] G.H. Markx, C.L. Davey, D.B. Kell, P. Morris, The dielectric permittivity at radio frequencies and the Bruggeman Probe: novel techniques for the on-line determination of biomass concentrations in plant cell cultures, J. Biotechnol. 20 (1991) 279–290.
[17] L. Davey, Y. Guan, R.B. Kemp, D.B. Kell, Real-time monitoring of the biomass content of animal cell cultures using dielectric spectroscopy, in: Animal Cell Technology Basic and Applied Aspects, K. Funatsu (Ed.), Proc. Japanese Association of Animal Cell Technology 81997, pp. 61–65.
[18] D.B. Kell, R.W. Todd, Dielectric estimation of microbial biomass using the Aber Instruments Biomass Monitor, Trends Biotechnol. 16 (1998) 149–150.
[19] G.H. Markx, C.L. Davey, D.B. Kell, To what extent is the value of the Cole–Cole $\alpha$ of the β-dielectric dispersion of cell suspensions accountable in terms of the cell size distribution?, Bioelectrochem. Bioenerg. 25 (1991) 195–211.
[20] C.L. Davey, H.M. Davey, D.B. Kell, On the dielectric properties of cell suspensions at high volume fractions, Bioelectrochem. Bioenerg. 28 (1992) 319–330.
[21] R. Pethig, Dielectric and Electronic Properties of Biological Materials, Wiley, Chichester, 1979.
[22] E.H. Grant, R.J. Sheppard, G.P. South, Dielectric Behaviour of Biological Molecules in Solution, Clarendon Press, Oxford, 1978.
[23] S. Takashima, Electrical Properties of Biopolymers and Membranes, Adam Hilger, Bristol, 1989.
[24] C.L. Davey, The Biomass Monitor Source Book, Aber Instruments, Aberystwyth, 1993.
[25] C.L. Davey, The Theory of the β-Dielectric Dispersion and its Use in the Estimation of Cellular Biomass, Aber Instruments, Aberystwyth, 1993.
[26] C.L. Davey, D.B. Kell, The dielectric properties of cells: what can they tell us about cellular physiology and the mechanisms of field/cell interactions?, in: Emerging Electromagnetic Medicine, Springer, Berlin, 1990, pp. 19–43.
[27] D.B. Kell, C.L. Davey, Conductimetric and impedimetric devices, in: Biosensors: A Practical Approach, Oxford Univ. Press, Oxford, 1990, pp. 125–154.
[28] H.P. Schwan, Determination of biological impedances, in: Physical Techniques in Biological Research VIB Academic Press, New York, 1963, pp. 323–407.
[29] H.P. Schwan, Electrode polarization impedance and measurements in biological materials, Ann. N.Y. Acad. Sci. 148 (1968) 191–209.
[30] B. Onaral, H.H. Sun, H.P. Schwan, Electrical properties of bioelectrodes, IEEE Trans. Biomed. Eng. BMI 31 (1984) 827–832.
[31] A.M. Woodward, A. Jones, Z. Xin-Zhu, J. Rowland, D.B. Kell, Rapid and non-invasive quantification of metabolic substrates in biological cell suspensions using non-linear dielectric spectroscopy with multivariate calibration and artificial neural networks: principles and applications, Bioelectrochem. Bioenerg. 40 (1996) 99–132.
[32] I. Cerckel, A. Garcia, V. Degouys, D. Dubois, L. Fabry, A.O.A. Miller, Dielectric-spectroscopy of mammalian-cells: 1. Evaluation of the biomass of Hela-Cell and CHO-Cells in suspension by low–frequency dielectric-spectroscopy, Cytotechnology 13 (1993) 185–193.
[33] M. Watanabe, T. Suzaki, A. Irimajiri, Dielectric behavior of the frog lens in the 100 Hz to 500 MHz range: simulation with an allocated ellipsoidal shells model, Biophys. J. 59 (1991) 139–149.
[34] C.L. Davey, D.B. Kell, The influence of electrode polarisation on dielectric spectra, with special reference to capacitive biomass measurements: II. Reduction in the contribution of electrode polarisation to dielectric spectra using a two-frequency method, Bioelectrochem. Bioenerg. 46 (1998) 105–114.
[35] C.L. Davey, D.B. Kell, The influence of electrode polarisation on dielectric spectra, with special reference to capacitive biomass measurements: I. Quantifying the effects on electrode polarisation of factors likely to occur during fermentations, Bioelectrochem. Bioenerg. 46 (1998) 91–103.
[36] M. Davies, Some Electrical and Optical Aspects of Molecular Behaviour, Pergamon Press, 1965.
[37] K.S. Cole, R.H. Cole, Dispersion and absorption in dielectrics: 1. Alternating current characteristics, J. Chem. Phys. 9 (1941) 341–351.